Strong dipole coupling in nonpolar nitride quantum dots due to Coulomb effects

K. Schuh' , S. Barthel, O. Marquardt, T. Hickel, J. Neugebauer, G. Czycholl, and F. Jahnke

Citation: Appl. Phys. Lett. **100**, 092103 (2012); doi: 10.1063/1.3688900
View online: http://dx.doi.org/10.1063/1.3688900
View Table of Contents: http://aip.scitation.org/toc/apl/100/9
Published by the American Institute of Physics

Strong dipole coupling in nonpolar nitride quantum dots due to Coulomb effects

K. Schuh,[1,a)] S. Barthel,[1] O. Marquardt,[2] T. Hickel,[3] J. Neugebauer,[3] G. Czycholl,[1] and F. Jahnke[1]
[1]*Institute for Theoretical Physics, University of Bremen, Germany*
[2]*Tyndall National Institute, Lee Maltings, Cork, Ireland and Max-Planck Institut für Eisenforschung, Düsseldorf, Germany*
[3]*Max-Planck Institut für Eisenforschung, Düsseldorf, Germany*

(Received 13 December 2011; accepted 7 February 2012; published online 27 February 2012)

Optical properties of polar and nonpolar nitride quantum dots (QDs) are determined on the basis of a microscopic theory which combines a continuum elasticity approach to the polarization potential, a tight-binding model for the electronic energies and wavefunctions, and a many-body theory for the optical properties. For nonpolar nitride quantum dots, we find that optical absorption and emission spectra exhibit a weak ground-state oscillator strength in a single-particle calculation whereas the Coulomb configuration interaction strongly enhances the ground-state transitions. This finding sheds new light on existing discrepancies between previous theoretical and experimental results for these systems, as a weak ground state transition was predicted because of the spatial separation of the corresponding electron and hole state due to intrinsic fields whereas experimentally fast optical transitions have been observed. © *2012 American Institute of Physics*. [http://dx.doi.org/10.1063/1.3688900]

Due to their wide range of emission frequencies,[1] nitride-based optoelectronic devices are of current interest. For applications in light emitters, fast radiative recombination rates are beneficial. However, a major drawback in nitrides is that this recombination is hindered by strong intrinsic fields due to the quantum-confined Stark effect which causes a separation of electrons and holes in nanostructures like quantum dots (QDs).

In two dimensional quantum wells, this effect can be avoided by enforcing a nonpolar growth direction,[2] which ensures the absence of fields in the confined direction. Since QD states are confined in all three dimensions, there is always a nonvanishing polarization potential and thus a spatial separation of electrons and holes. Nevertheless, experimental results indicate increased recombination rates in nonpolar nitride QDs in comparison to polar QDs.[3]

Recent theoretical studies have investigated the influence of intrinsic fields on the single-particle states concerning the sign of piezoelectric constants,[4] geometry,[5] and concentration.[6] These studies revealed only a marginal spatial overlap of the electron and hole single-particle ground state in nonpolar QDs implying a very slow recombination due to dipole transitions between the ground states. This is mainly caused by the larger spatial dimension of the nonpolar grown QDs in the direction of the fields, so that the spatial separation is even larger in these dots in comparison to the polar ones.

The aim of this paper is to determine optical properties of polar and nonpolar nitride QDs on the basis of electronic state calculations and the inclusion of electron-hole-pair Coulomb interaction. As shown in Ref. 7, single-particle calculations like Hartree-Fock (HF) omit important correlation effects. In order to include correlation effects, the excitonic states are obtained by a full configuration interaction (FCI) calculation using product states of all electron and hole single-particle QD eigenfunctions as a basis, which is obtained by a tight-binding (TB) calculation in this work. Note, that the FCI method is well established and was extensively applied to QD systems using a basis obtained by e.g., effective mass,[8] $k \cdot p$,[9] TB (Ref. 10), and emipirical pseudopotential[11] models. Before employing this many-body procedure, we discuss the calculation and optical properties of the localized single-particle QD states.

We consider pure InN/GaN lens-shaped QDs of 7.7 nm diameter and 3.1 nm height for the polar growth direction on a wetting-layer (WL) with a thickness of 2 lattice constants.[12–14] The WL states are not considered in the FCI calculation, since they do not significantly influence the lower QD state transitions due to their rather large energy separation. Though it is known that also the shape and the size of the QDs may depend on the growth direction,[15] we assume the same QD geometry for the nonpolar growth direction (with the restriction that the modeling in the different crystal orientations requires a shift of the QD boundaries of about 10%) to focus on the effect of the built-in field orientation on the optical properties.

The single-particle states of these nitride semiconductor QDs are calculated by employing the empirical tight binding model of Ref. 16. We use supercells suitable for the nanostructure, i.e., a hexagonal one for the polar QD and a cuboid for the nonpolar QD, in combination with periodic boundary conditions and the folded-spectrum method[17] for diagonalization. This model provides a realistic description of the bulk bandstructure throughout the full Brillouin zone using the sp^3-basis and hopping matrix elements up to second nearest neighbors. Recent G_0W_0 data[16,18] serve as input for the parametrization scheme of the bulk matrix elements. The weak spin-orbit splitting of about 5 meV for InN (Ref. 19) is neglected.

a)Electronic mail: kschuh@itp.uni-bremen.de.

To calculate the polarization potential, the elastic energy in the QD and the surrounding matrix has been minimized with respect to the displacements in a second-order continuum elasticity model. The strain tensor was then obtained from the displacements and enters the polarization vector, in first-order piezoelectric contributions, together with the spontaneous polarization. By solving the Poisson equation, the polarization potential is determined. These calculations have been performed in a plane-wave framework, for details see Ref. 20. In order to incorporate the polarization potential properly in the TB calculations, we employ an interpolation to the corresponding lattice and perform a symmetrization to avoid any artificial symmetry spoiling.

The nanostructure's Hamiltonian is constructed by using the empirical bulk matrix elements for each material at the respective lattice sites $\vec{R}$. The electrostatic potential energy is then added as an on-site contribution to the tight-binding Hamiltonian according to the central-cell correction.[21] By diagonalizing this real-space Hamiltonian exactly, one obtains the bound QD eigenstates $|\alpha\rangle$. To ensure that all QD states are included in the FCI, we calculate all eigenfunctions up to the WL band edges. They are approximated by solving semianalytically the tight-binding Hamiltonian (not shown) of the two-dimensional, translational invariant WL problem. We end up with 25 (8) electronic and 90 (96) hole bound QD states in the nonpolar (polar) QD, which are considered in the FCI.

The intrinsic fields and the QD geometry are depicted in Fig. 1 for the polar (c-plane) and nonpolar (m-plane) growth direction. As expected, these fields are reduced in the nonpolar growth direction, since the spontaneous polarization part is weaker. The maximum potential energy difference is changed by about 100 meV from 488 meV (polar) to 384 meV (nonpolar) which causes a lower transition energy for the polar QDs, since the ground states are bound more strongly. In both cases, the fields are rather strong, so that the single-particle calculation yields large spatial separations for the lowest electron and hole states with a marginal overlap. This fact can clearly be seen in the left panels of Fig. 2, where the probability density of the lowest electron and hole QD states are depicted as insets. In the polar case, the spatial separation between electron and hole states exists also for excited hole states up to 100 meV above the ground state, whereas in the nonpolar case, the excited hole states have a considerably larger overlap with the electronic states.

These additional spatial overlaps indicate increasing dipole matrix elements

$$\vec{d}_{\alpha\beta} = \langle \alpha | e\hat{R} | \beta \rangle$$

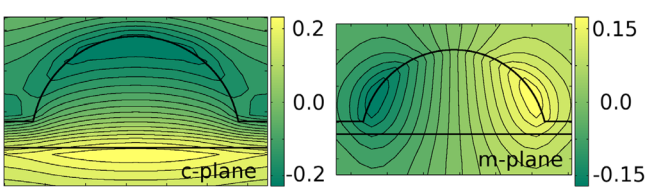

FIG. 1. (Color online) Intrinsic electrostatic potential energy in eV for the polar (c-plane) and the nonpolar (m-plane) QD. The shape of the QDs is indicated by the black lines.

with e being the elementary charge. They are calculated by using the envelope representation of the spatial operator $\hat{R}$ according to Ref. 22. These matrix elements enter directly the linear optical spectra by employing Fermi's golden rule

$$I(E) = \frac{2}{\hbar} \sum_{\alpha,\beta} |\vec{d}_{\alpha\beta}|^2 \frac{\Delta}{\Delta^2 + (E_\alpha + E_\beta - E)^2} \tag{1}$$

including a Lorentzian broadening of $\Delta = 10\,\text{meV}$ as observed in Ref. 14 for elevated temperatures. The broadening may be interpreted physically as simulating the influence of all inelastic scattering processes not explicitly taken into account.

Due to the high density of states for the holes, there are many possible transitions between the electron ground state and several hole states in a spectrally small area. The resulting single-particle spectra for the non-interacting system are shown in the left panels of Fig. 2. For the polar QD, the ground-state transition is dominant. Since the absorption is composed of two degenerate hole states, the emission of the ground state exciton (blue dotted line) is only half as high as the absorption (red solid line). Despite the rather large hole density of states near the ground-state energy, there are only few much weaker transitions in the energetic vicinity because most of the states are dark or possess a weak dipole coupling to the electron ground state due to the C_{6v}-symmetry of the QD. Further, appreciable contributions from excited states are spectrally well separated resulting in this detached peak structure.

In contrast, optical transitions between the lowest states of the nonpolar QD are much weaker and also the first exited hole states do not contribute significantly. Thus, the emission of the ground state transition is considerably reduced in comparison to the polar QD. Remarkably, for the nonpolar QD, there are strong transitions of the electronic ground state with excited hole states. Moreover, most states are optically active due to the lower symmetry. Thus, there is a quasi-continuous absorption in the vicinity of the ground state transition because of the large density of states instead of discrete spectral features as observed in the spectrum of the polar QD. The absorption above the ground state transition increases considerably due to the additional dipole transitions. At energies about 80 meV above the ground state transition, the absorption is even higher than for the ground states of the polar QD. In both cases, the excited electron states do not contribute at the transition energies shown.

The excitonic states, i.e., many-body states that include one electron-hole pair, are obtained by FCI calculations using all product states as a basis. The many-body Hamiltonian

$$\hat{H}_X = \sum_\alpha E_\alpha \hat{e}_\alpha^\dagger \hat{e}_\alpha + \sum_\beta E_\beta \hat{h}_\beta^\dagger \hat{h}_\beta - \sum_{\alpha\beta\alpha'\beta'} V_{\alpha\beta\beta'\alpha'}^{ehhe} \hat{e}_\alpha^\dagger \hat{e}_{\alpha'} \hat{h}_\beta^\dagger \hat{h}_{\beta'}$$

includes, besides the single-particle energies E, the direct and exchange Coulomb interaction. The small electron-hole exchange (V^{eheh}) as well as processes that change the number of carriers are excluded. Since we are only interested in the excitonic states, there is no electron-electron or hole-hole interaction present. The Coulomb matrix elements

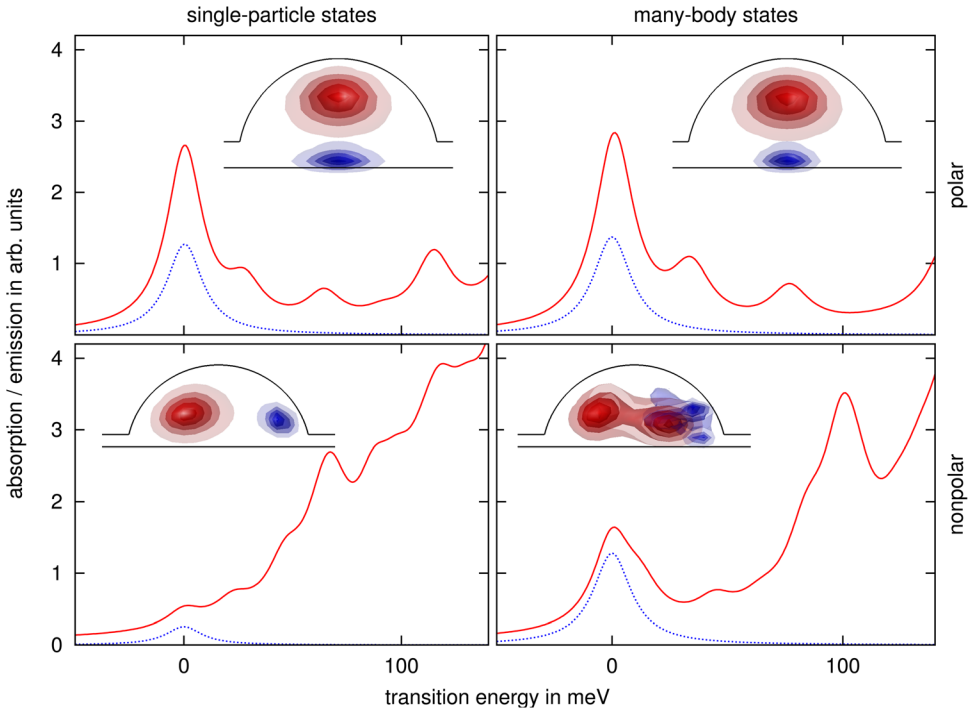

FIG. 2. (Color online) Absorption spectra of the empty system (red solid line) and emission spectra of the ground state exciton (blue dotted line) based on the single particle states, i.e., without many-body effects, (left panels) and including many-body effects (right panels) for polar (upper panels) and nonpolar (lower panels) QDs versus photon energy relative to the respective ground-state transition. The insets show the isosurfaces of equal probability density (0.9 to 0.1) for the electron (red) and hole (blue) single-particle ground states and excitonic many-body ground state, respectively. For the polar QD the electronic part is located in the upper side and for the nonpolar QD in the left side. For the nonpolar QD with many-body interaction, the electronic part has a barbell-shaped form and an enhanced overlap with the hole part.

$$V^{ehhe}_{\alpha\beta\beta'\alpha'} = \frac{1}{2V}\sum_{\vec{q}}\frac{e^2}{\epsilon q^2}\langle\alpha|e^{i\vec{q}\vec{R}}|\alpha'\rangle\langle\beta|e^{-i\vec{q}\vec{R}}|\beta'\rangle$$

are calculated in the Fourier-space and include the elementary charge e, the permittivity ϵ, and the system Volume V, for further details see Ref. 23. By a diagonalization of the Hamiltonian $\hat{H}_X$, one obtains the excitonic states

$$|\psi_X\rangle = \sum_{\alpha\beta} c_X^{\alpha\beta}\hat{e}^\dagger_\alpha\hat{h}^\dagger_\beta|0\rangle$$

as linear combinations of the product states with the coefficients $c_X^{\alpha\beta}$. There are in the case of the nonpolar QD 2250 and in the polar case 768 product states. This allows to solve the eigenvalue problem of the Coulomb interaction exactly without further restrains. In particular, all Coulomb correlations within the chosen basis are included. For further details, see Refs. 22, 24 and 25. In an analogous way, the dipole strength of the excitonic states is derived by

$$\vec{d}_X = \sum_{\alpha\beta} c_X^{\alpha\beta}\vec{d}_{\alpha\beta},$$

which allows the calculation of the excitonic spectra in the same manner as the single-particle ones by Fermi's golden rule (1). The spectra are presented in the right panels of Fig. 2. Due to the Coulomb interaction, the ground-state transitions are shifted by 70 meV for the polar QD and 99 meV for the nonpolar QD. While the emission as well as absorption strength of the ground state transition is only slightly changed in the case of the polar QD, a strong enhancement of the ground-state transition can be seen in the spectra of the nonpolar QD. Now, the nonpolar QD ground-state transition has about the same oscillator strength as the polar QD due to contributions from excited single-particle states with larger dipoles.

The physical origin of this change for the nonpolar QD orientation can be identified by comparing the electron and hole probability densities of the ground state for the single-particle calculation (left insets) and the FCI calculation including excitonic Coulomb effects (right insets). The spatial separation of electron and hole gives rise to a small dipole matrix element in the single particle case whereas the attractive electron-hole Coulomb interaction increases the overlap in the nonpolar case. Further analysis (not shown) reveals that the electronic many-body ground state has notable contributions from the five lowest single-particle states. Interestingly, the hole many-body ground state has considerable contributions from a large number of single-particle states.

Carrying out the same analysis for the polar QD orientation, the corresponding many-body ground state is mainly constructed from the lowest electronic single-particle state and the two degenerate lowest hole single-particle states. Thus, the probability densities of the single-particle and many-body ground states differ only slightly. This suggests that a truncation of the single-particle basis after the lowest states entering the FCI can be justified in the polar QD orientation for an exciton, while in the nonpolar QD orientation, this approximation does not hold, since it prevents the formation of the correct many-body ground state. Quantitatively, this effect is related to the spatial separation of the excited states. Due to the about 2.5 times larger electrostatic field strength in the polar QD also excited electron and hole states are separated, while in the nonpolar case, there is an increased overlap of the excited states. This allows for an increased electron-hole interaction leading to strong contributions of excited single-particle states to the excitonic ground state.

In summary, our results for the lowest *single-particle states* in polar and nonpolar nitride QDs confirm previous studies[4,5] showing a drop in the dipole matrix elements by

changing the geometry from a polar to a nonpolar facet. However, conclusions about the electron-hole overlap and the resulting optical transition efficiencies require the inclusion of Coulomb interaction between various single-particle states. In order to describe the optical properties of the ground-state transition of the investigated InN/GaN QDs, we used Coulomb FCI calculations that lead to a significantly increased ground state dipole transition for the nonpolar InN/GaN QD. This effect is caused by a strong mixture of many single-particle states. In contrast, Coulomb interaction does not lead to a qualitative change in the spectra for the polar orientation and provides essentially an energetic shift. As a result, the excitonic ground states of both nitride QD orientations have about the same dipole strength.

This work was supported by the Deutsche Forschungsgemeinschaft. The authors thank Paul Gartner for fruitful discussions.

[1]S. Nakamura, Science **281**, 956 (1998).
[2]C. Wetzel, M. Zhu, J. Senawiratne, T. Detchprohm, P. Persans, L. Liu, E. Preble, and D. Hanser, J. Cryst. Growth **310**, 3987 (2008).
[3]S. Founta, F. Rol, E. Bellet-Amalric, J. Bleuse, B. Daudin, B. Gayral, H. Mariette, and C. Moisson, Appl. Phys. Lett. **86**, 171901 (2005).
[4]S. Schulz, A. Berube, and E. P. O'Reilly, Phys. Rev. B **79**, 081401 (2009).
[5]O. Marquardt, T. Hickel, and J. Neugebauer, J. Appl. Phys. **106**, 083707 (2009).
[6]S. Schulz and E. P. O'Reilly, Phys. Status Solidi C **7**, 80 (2010).
[7]M. Braskén, M. Lindberg, D. Sundholm, and J. Olsen, Phys. Rev. B **61**, 7652 (2000).
[8]Y. Z. Hu, M. Lindberg, and S. W. Koch, Phys. Rev. B **42**, 1713 (1990).
[9]A. Schliwa, M. Winkelnkemper, and D. Bimberg, Phys. Rev. B **79**, 075443 (2009).
[10]S. Schulz, S. Schumacher, and G. Czycholl, Phys. Rev. B **73**, 245327 (2006).
[11]A. Franceschetti, H. Fu, L. W. Wang, and A. Zunger, Phys. Rev. B **60**, 1819 (1999).
[12]A. Rosenauer, T. Mehrtens, K. Müller, K. Gries, M. Schowalter, P. V. Satyam, S. Bley, C. Tessarek, D. Hommel, K. Sebald *et al.*, Ultramicroscopy **111**, 1316 (2011).
[13]C. Tessarek, S. Figge, T. Aschenbrenner, S. Bley, A. Rosenauer, M. Seyfried, J. Kalden, K. Sebald, J. Gutowski, and D. Hommel, Phys. Rev. B **83**, 115316 (2011).
[14]K. Sebald, J. Kalden, H. Lohmeyer, and J. Gutowski, Phys. Status Solidi B **248**, 1777 (2011).
[15]X. Yang, M. Arita, S. Kako, and Y. Arakawa, Appl. Phys. Lett. **99**, 061914 (2011).
[16]D. Mourad, S. Barthel, and G. Czycholl, Phys. Rev. B **81**, 165316 (2010).
[17]L.-W. Wang and A. Zunger, J. Chem. Phys. **100**, 2394 (1994).
[18]Q. Yan, P. Rinke, M. Winkelnkemper, A. Qteish, D. Bimberg, M. Scheffler, and C. G. Van de Walle, Semicond. Sci. Technol. **26**, 014037 (2011).
[19]I. Vurgaftman and J. R. Meyer, J. Appl. Phys. **94**, 3675 (2003).
[20]O. Marquardt, S. Boeck, C. Freysoldt, T. Hickel, and J. Neugebauer, Comput. Phys. Commun. **181**, 765 (2010).
[21]J. C. Slater and G. F. Koster, Phys. Rev. **94**, 1498 (1954).
[22]S. Schulz, D. Mourad, and G. Czycholl, Phys. Rev. B **80**, 165405 (2009).
[23]J. Seebeck, M. Lorke, S. Schulz, K. Schuh, P. Gartner, and F. Jahnke, Phys. Status Solidi B **248**(8), 1871 (2011).
[24]N. Baer, P. Gartner, and F. Jahnke, Eur. Phys. J. B **42**, 213 (2004).
[25]N. Baer, S. Schulz, P. Gartner, S. Schumacher, G. Czycholl, and F. Jahnke, Phys. Rev. B **76**, 75310 (2007).